

### Quasiperiodic dynamics for a generalized third-order Fibonacci series

M. K. Ali and Godfrey Gumbs

*Department of Physics, University of Lethbridge, Lethbridge, Alberta, Canada T1K 3M4*

(Received 28 April 1988)

A simple quasiperiodic arrangement made up of three building blocks is introduced in terms of a third-order Fibonacci series. We obtain a dynamical system for the series of transfer matrices for the one-dimensional Schrödinger equation and derive the reduced dynamical map of the traces. This map has some unique features compared with the second-order Fibonacci series.

There has been considerable interest in the discrete Schrödinger equation with a quasiperiodic potential. This problem was originally proposed by Kohmoto, Kadanoff, and Tang<sup>1</sup> and Ostlund *et al.*<sup>2</sup> The interest in this problem devolves upon its connection with a simple dynamical system for which rigorous analytical results and detailed numerical results could be obtained with relative ease.<sup>1-14</sup> From a physical point of view, the one-dimensional quasiperiodic Schrödinger equation is interesting since it is, in some sense, the projection of a quasicrystal onto a line. Much of our understanding of quasicrystal structures such as Al<sub>0.86</sub>Mn<sub>0.14</sub> is based on a detailed study of a two-dimensional tiling pattern discovered by Penrose<sup>15</sup> and described by Gardner.<sup>16</sup> These structures are like mosaics with more than one line shape. Hence, the potential and hopping matrix elements of the discrete Schrödinger equation could be constructed according to any quasiperiodic sequence. Most of the theoretical and numerical calculations, however, have been carried out for the Fibonacci series with the golden mean. Recently, the authors<sup>17,18</sup> described two classes of quasiperiodic sequences and obtained the dynamical maps for these arrangements. The building blocks of the sequences introduced in Refs. 17 and 18 form a binary string. In this paper, we study the discrete Schrödinger equation with a *ternary* string and derive the dynamical map for the traces. We also compare the trace map for the ternary sequence with a new binary array. By numerical calculations of the trace map, we find that the orbits of the ternary string escape to infinity fairly rapidly indicating a very strong repeller.

The discrete Schrödinger equation for the diagonal model is given by

$$\begin{pmatrix} \psi_{l+1} \\ \psi_l \end{pmatrix} = \underline{M}(l) \begin{pmatrix} \psi_l \\ \psi_{l-1} \end{pmatrix}, \tag{1}$$

where  $\psi_l$  denotes the tight-binding wave function of the  $l$ th lattice site and  $\underline{M}(l)$  is a transfer matrix defined by

$$\underline{M}(l) = \begin{pmatrix} E - V_l & -1 \\ 1 & 0 \end{pmatrix}. \tag{2}$$

By successively applying the transfer matrices, we obtain the wave function at arbitrary sites. Let us define  $\underline{M}_l \equiv \underline{M}(F_l)\underline{M}(F_l-1)\dots\underline{M}(2)\underline{M}(1)$ , where  $F_l$  is a third-order Fibonacci number defined as the sum of the three preceding numbers with  $F_{l+1} = F_{l-2} + F_{l-1} + F_l$  for

$l \geq 2$  and  $F_0 = F_1 = F_2 = 1$  (Ref. 19). In the limit as  $l \rightarrow \infty$ ,  $F_{l+1}/F_l$  tends to the mean value  $\sigma_l = \frac{1}{3}(1 + \gamma_+^{1/3} + \gamma_-^{1/3})$ , where  $\gamma_{\pm} \equiv 19 \pm 297^{1/2}$ . The matrix  $\underline{M}_l$  generates a wave function at a Fibonacci number site. For the three building blocks  $A$ ,  $B$ , and  $C$  the sequence is constructed by  $S_{l+1} = \{S_{l-2}S_{l-1}S_l\}$  for  $l \geq 3$  with  $S_1 = \{C\}$ ,  $S_2 = \{ABC\}$ , and  $S_3 = \{BCABC\}$ . Alternatively, the sequence can be generated by the inflation transformation  $C \rightarrow ABC$ ,  $B \rightarrow C$ , and  $A \rightarrow B$ .  $\underline{M}_l$  satisfies

$$\underline{M}_{l+1} = \underline{M}_{l-2}\underline{M}_{l-1}\underline{M}_l, \tag{3}$$

for  $l \geq 3$ . The energy spectrum is obtained by looking for energies whose corresponding wave functions  $\psi_l$  do not grow as the value of  $l$  increases. Since the determinant of  $\underline{M}_l$  is unity, the condition that  $E$  lies in the spectrum is that the trace satisfies the relation  $|\text{Tr}\underline{M}_l| < 2$ . We now obtain the recursion relation for  $x_l = \frac{1}{2}\text{Tr}\underline{M}_l$ . It can be shown by a careful manipulation of Eq. (3) that

$$\underline{M}_{l+1} + \underline{M}_l^{-1} = \underline{M}_{l-2}\underline{M}_{l-1}(\underline{M}_l + \underline{M}_l^{-1}). \tag{4}$$

Since  $\underline{M}_l$  is a sequence of  $2 \times 2$  matrices with determinant equal to unity, it is a simple matter to show upon taking the trace of Eq. (4) that

$$x_{l+1} = 4x_l G_l - x_{l-3}, \tag{5a}$$

where  $G_l \equiv \frac{1}{4}\text{Tr}(\underline{M}_{l-2}\underline{M}_{l-1})$ . After a straightforward calculation, we find that  $G_l$  has a recursion relation given by

$$G_l = x_{l-1}x_{l-2} - G_{l-2}, \tag{5b}$$

where

$$x_1 = \frac{1}{2}\text{Tr}(C), \quad x_0 = \frac{1}{2}\text{Tr}(B),$$

$$x_{-1} = \frac{1}{2}\text{Tr}(A), \quad x_2 = 4x_1x_0x_{-1} - x_1 - x_0 - x_{-1},$$

$$G_0 = \frac{1}{2}, \quad G_1 = x_{-1}x_0 - \frac{1}{2}.$$

Equations (5) define a renormalization map in a six-dimensional space. It has the trivial fixed points  $x_l = 0, \pm 1$ , with unit cycle. Also for  $x_1 = x_0 = x_{-1} = x$  with  $|x| < 1$ , calculation shows that  $|x_l| < 1$  for all values of  $l$ . For example, when the initial points are at  $x = \pm 2^{1/2}$ , the trace-map as well as the matrices have an eight-cycle, i.e.,  $x_l = x_{l+8}$  and  $\underline{M}_l = \underline{M}_{l+8}$ . We have carried out an extensive search for those initial points  $x_1, x_0$ , and  $x_{-1}$

which give rise to periodic and aperiodic orbits inside the cube with its center at the origin and with sides of length equal to two. We were not able to find any points, besides the ones along the diagonal, that give rise to bounded orbits. This does not necessarily mean that there are no other points which would initiate bounded orbits. The result of our numerical calculations is that the map defined in Eqs. (5) for the third-order Fibonacci lattice has far fewer orbits than the second-order Fibonacci lattices studied so far.<sup>17,18</sup> As a matter of fact, the dynamical maps for the trace of the transfer matrices satisfying the recursion relation  $\underline{M}_{j+1} = \underline{M}_{j-1} \underline{M}_j^n$  where  $n = 1, 2, \dots$  have been found to have several cyclic orbits. More interestingly, the two-dimensional map generated from  $\underline{M}_{j+1} = \underline{M}_{j-1}^2 \underline{M}_j$  has been shown<sup>17</sup> to have an astonishingly larger number of initial points which produce bounded (cyclic or quasi-periodic) orbits. This latter map is one example of a general class of sequences generated by the rule  $\underline{M}_{j+1} = \underline{M}_{j-1}^m \underline{M}_j$ . We have derived the new dynamical map for the case when  $m = 3$ . By defining a three-dimensional vector  $\underline{l} = (x_l, y_l, z_l)$ , this map is nonlinear and given explicitly by

$$\begin{aligned} x_{l+1} &= 2x_l y_l + z_l, \\ y_{l+1} &= (4x_l^2 - 3)x_l, \\ z_{l+1} &= 2x_l z_l + y_l, \end{aligned} \quad (6)$$

where  $x_1 = \frac{1}{2} \text{Tr}M(A)$ ,  $x_2 = \frac{1}{2} \text{Tr}M(B)$  for  $M$  defined by Eq. (2). With the use of numerical methods, we searched for all those initial points which produce bounded orbits for the map in Eq. (6). Our results for a subset of these initial points are shown in Fig. 1 and have some similarity with the map<sup>17</sup> corresponding to  $m = 2$ . Thus the third-order Fibonacci map is unique among the second-order maps studied so far. We have not been able to obtain an

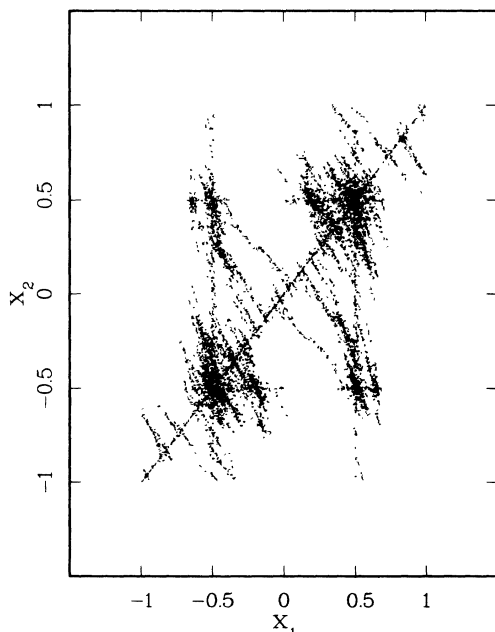


FIG. 1. The set of initial points with coordinates  $x_1$  and  $x_2$  which produce bounded orbits for the map defined in Eq. (6).

invariant for the map in Eqs. (5). By way of investigation, we have shown that there is no invariant of polynomial types with quadratic and cubic terms as in the sequences investigated in Ref. 17. Numerical calculations show that  $x_l$  gets large more quickly than the binary Fibonacci series.<sup>17</sup> This rapid rate of growth of  $|x_l|$  with increasing  $l$  implies a very strong repeller on the Fibonacci sublattice.

We now turn to the nondiagonal tight-binding model for which the discrete Schrödinger equation is given by

$$t_{l+1} \psi_{l+1} + t_l \psi_{l-1} = E \psi_l. \quad (7)$$

Equation (7) can be written as

$$\Psi(l+1) = \underline{M}(l+1, l) \Psi(l),$$

where  $\Psi(l)$  is a column vector with  $\psi_l$  in the first row and  $\psi_{l-1}$  in the second row. The transfer matrix is

$$\underline{M}(l+1, l) \equiv \begin{pmatrix} E/t_{l+1} & -t_l/t_{l+1} \\ 1 & 0 \end{pmatrix}. \quad (8)$$

This off-diagonal model is more complicated than the diagonal model in Eq. (1) since  $\underline{M}(l+1, l)$  depends on two bonds. However, we could obtain closed form analytic results for the wave function at the third-order Fibonacci lattice sites by defining a transfer matrix  $\underline{M}_j$  given recursively by Eq. (3) with initial conditions

$$\begin{aligned} \underline{M}_1 &= \underline{M}(c, c), \\ \underline{M}_2 &= \underline{M}(c, a) \underline{M}(a, b) \underline{M}(b, c), \\ \underline{M}_3 &= \underline{M}(b, c) \underline{M}(c, b) \underline{M}_2. \end{aligned} \quad (9)$$

$\underline{M}_j$  has determinant equal to unity with the trace map

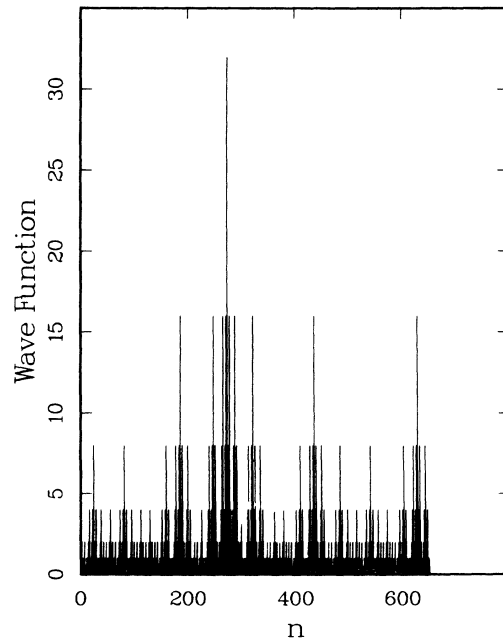


FIG. 2. The wave function at the center of the spectrum  $E = 0$  of the nondiagonal model in Eq. (7) with hopping matrix elements  $a = 2$ ,  $b = 1$ , and  $c = \frac{1}{2}$ .

given by Eqs. (5) and the initial conditions

$$\begin{aligned} G_2 &= \frac{1}{4} \text{Tr}[\underline{M}(b,c) \underline{M}(c,b)], \\ G_3 &= x_1 x_2 - \frac{1}{4} \text{Tr}[\underline{M}(a,b) \underline{M}(b,a)], \\ x_4 &= 4x_3 G_3 - E/(2b). \end{aligned} \quad (10)$$

When  $E=0$ ,  $x_l=0$  for all values of  $l$  and the transfer matrices form a four-cycle orbit with  $\underline{M}_l = \underline{M}_{l+4}$ . Interestingly, although the trace is zero on the Fibonacci sublattice when the energy is at the center of the band, the wave function is finite on the real lattice and even has a self-similar structure. None of the second-order Fibonacci series have this unexpected behavior. For example, the matrix map for the Fibonacci series with the golden mean has a six-cycle orbit at the center of the band but the trace map is not zero.<sup>14</sup> Figure 2 is an example of the wave function for the nondiagonal model when  $E=0$ . The wave function grows algebraically.

Next, we calculate the  $N$  dependence of the resistance for a chain of length  $N$ . We recall the expression for the resistance, defined as the ratio between the reflection and the transmission coefficients.<sup>20</sup> It is given by<sup>12,21</sup>

$$\rho_N = \frac{1}{4\sin^2 k} [\|\underline{M}_N\|^2 + 2(\cos k)(M_N^{11} - M_N^{22})(M_N^{12} - M_N^{21}) - 4(\cos^2 k)M_N^{12}M_N^{21} - 2], \quad (11)$$

where  $\|\underline{M}_N\|^2$  denotes the sum of the squares of the elements of the  $2 \times 2$  matrix  $\underline{M}_N \equiv \prod_{l=1}^N \underline{M}(l)$ . We also define the energy in terms of the wave vector  $k$  by  $E = 2t_c \cos k$ , where the hopping matrix elements are equal to  $t_c$  outside the disordered segment  $1 \leq l \leq N$ . In Fig. 3, a numerical example is presented for the resistance of a third-order Fibonacci lattice. The resistance  $\rho_N$  vanishes for certain values of  $N$ , corresponding to total transmission. These calculations provide strong evidence for algebraic localization and are worth investigating experimentally. Comparing these results with those of Schneider,

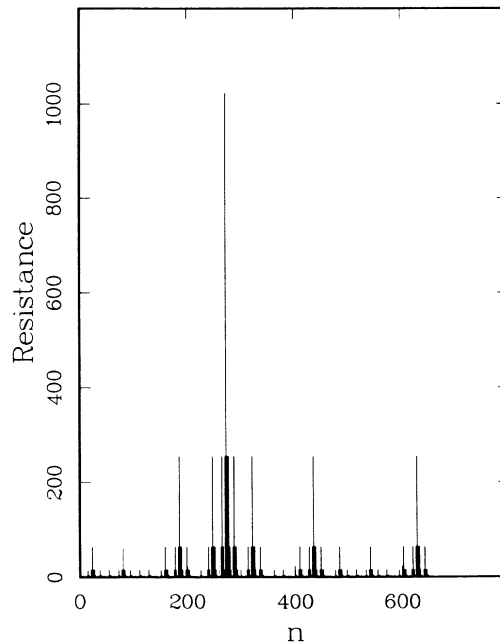


FIG. 3.  $N$  dependence of the resistance for  $E=0$  and  $a=2$ ,  $b=1$ , and  $c=\frac{1}{2}$ .

Politi, and Würtz<sup>12</sup> we see that the overall structure for the resistance of a third-order Fibonacci lattice is similar to the Fibonacci lattice with the golden mean. That is, by adding a third element in the building blocks we do not destroy the unique features in the resistance of a quasi-periodic array.

This work is based on research supported by the Natural Sciences and Engineering Research Council of Canada. One of us (G.G.) also thanks the Alexander von Humboldt-Stiftung for additional financial support.

<sup>1</sup>M. Kohmoto, L. P. Kadanoff, and C. Tang, Phys. Rev. Lett. **50**, 1870 (1983).

<sup>2</sup>S. Ostlund, R. Pandit, D. Rand, H. J. Schellnhuber, and E. D. Siggia, Phys. Rev. Lett. **50**, 1873 (1983).

<sup>3</sup>S. Ostlund and R. Pandit, Phys. Rev. B **29**, 1394 (1984).

<sup>4</sup>M. Kohmoto, B. Sutherland, and C. Tang, Phys. Rev. B **35**, 1020 (1987).

<sup>5</sup>M. Kohmoto and Y. Oono, Phys. Lett. **102A**, 145 (1984).

<sup>6</sup>J. B. Sokoloff, Phys. Rev. B **22**, 5823 (1980).

<sup>7</sup>B. Sutherland, Phys. Rev. Lett. **57**, 770 (1986).

<sup>8</sup>D. R. Hofstadter, Phys. Rev. B **14**, 2239 (1976).

<sup>9</sup>W. Craig, Commun. Math. Phys. **88**, 113 (1983).

<sup>10</sup>M. Casdagli, Commun. Math. Phys. **107**, 295 (1986).

<sup>11</sup>F. Delyon and D. Petritis, Commun. Math. Phys. **103**, 441 (1986).

<sup>12</sup>T. Schneider, A. Politi, and D. Würtz, Z. Phys. B **66**, 469 (1987).

<sup>13</sup>B. Simon, Adv. Appl. Math **3**, 463 (1982).

<sup>14</sup>M. Kohmoto and J. R. Banavar, Phys. Rev. B **34**, 563 (1986).

<sup>15</sup>R. Penrose, Bull. Inst. Math. Appl. **10**, 266 (1974).

<sup>16</sup>M. Gardner, Sci. Am. **236**, 110 (1977).

<sup>17</sup>G. Gumbs and M. K. Ali, Phys. Rev. Lett. **60**, 1081 (1988).

<sup>18</sup>G. Gumbs and M. K. Ali (unpublished).

<sup>19</sup>M. R. Schröder, *Number Theory in Science and Communication* (Springer, New York, 1984), Chap. 5.

<sup>20</sup>R. Landauer, Philos. Mag. **21**, 863 (1970).

<sup>21</sup>A. D. Stone, J. D. Joannopoulos, and D. J. Chadi, Phys. Rev. B **24**, 5583 (1981).